

# Systematic variation in the temperature dependence of bacterial carbon use efficiency

Thomas P. Smith<sup>1,\*</sup>, Tom Clegg<sup>1</sup>, Thomas Bell<sup>1</sup>, and Samrāt Pawar<sup>1,\*</sup>

<sup>1</sup>Department of Life Sciences, Imperial College London, Silwood Park, Ascot, Berkshire SL5 7PY, UK

\*To whom correspondence should be addressed:

thomas.smith1@imperial.ac.uk; s.pawar@imperial.ac.uk

Understanding the temperature dependence of carbon use efficiency (CUE) is critical for understanding microbial physiology, population dynamics, and community-level responses to changing environmental temperatures<sup>1,2</sup>. Currently, microbial CUE is widely assumed to decrease with temperature<sup>3,4</sup>. However, this assumption is based largely on community-level data, which are influenced by many confounding factors<sup>5</sup>, with little empirical evidence at the level of individual strains. Here, we experimentally characterise the CUE thermal response for a diverse set of environmental bacterial isolates. We find that contrary to current thinking, bacterial CUE typically responds either positively to temperature, or has no discernible temperature response, within biologically meaningful temperature ranges. Using a global data-synthesis, we show that our empirical results are generalisable across a much wider diversity of bacteria than have previously been tested. This systematic variation in the thermal responses of bacterial CUE stems from the fact that relative to respiration rates, bacterial population growth rates typically respond more strongly to temperature, and are also subject to weaker evolutionary constraints. Our results provide fundamental new insights into microbial physiology, and a basis for more accurately modelling the effects of shorter-term thermal fluctuations as well as longer-term climatic warming on microbial communities.

26

27 The efficiency with which bacterial populations convert organic carbon into biomass, generally termed  
28 Carbon Use Efficiency (CUE), is a key physiological measure that ultimately determines the rate at  
29 which whole microbial communities decompose organic matter and release CO<sub>2</sub><sup>1</sup>. Therefore, CUE is a  
30 key parameter in global carbon cycle models<sup>2,6</sup>, as well as models of soil biogeochemical processes<sup>3,7,8</sup>  
31 and marine particle export<sup>9</sup>. CUE is typically quantified as the ratio of carbon allocated to biomass  
32 production relative to the total carbon assimilated<sup>1,10</sup>:

$$33 \quad \text{CUE} = \frac{\text{Growth rate}}{\text{Growth rate} + \text{Respiration rate}}. \quad (1)$$

34 The denominator of this quantity is the sum of rates of carbon allocation to growth and respiration,  
35 a common approximation where direct measurements of uptake are not feasible<sup>1,11,12,13</sup>. High CUE  
36 values imply increased biomass production (sequestration) relative to CO<sub>2</sub> release due to respiration,  
37 and vice versa<sup>1</sup>. Microbial CUE varies with environmental conditions such as resource stoichiometry  
38 and availability<sup>11</sup>, and physical parameters such as pH and temperature<sup>13,14</sup>. CUE values reported from  
39 environmental samples are therefore generally much lower than may be expected from theoretical calcula-  
40 tions<sup>10</sup>, as microbial communities are very rarely operating under conditions for optimal growth efficiency.  
41 The response of microbial CUE to changes in environmental temperature is particularly important, both  
42 for understanding how microbial communities respond to spatial and temporal variation in temperature,  
43 as well as for predicting the effects of climate change on carbon cycling.

44 Currently, models of organic matter decomposition typically assume a decrease in microbial CUE with  
45 temperature<sup>3,4,15</sup>. This is based on the premise that microbial respiration rate displays a stronger thermal  
46 sensitivity than growth rate<sup>1,4</sup>, implying that growth efficiency declines with temperature. However,  
47 results from empirical studies in both soil<sup>16,17</sup> and aquatic systems<sup>1,14,18</sup> are ambiguous, with studies  
48 variously finding decreases<sup>7</sup>, increases<sup>12</sup>, or little to no change in CUE with temperature<sup>19,20,21</sup>. Recent  
49 work at the level of single bacterial strains has also challenged this generalisation, finding variable CUE  
50 thermal responses between taxa<sup>13</sup>. However, most previous studies have focused on the CUE of whole  
51 microbial consortia in environmental samples, permitting limited mechanistic understanding of these  
52 responses. This is because temperature-driven community composition changes are expected to influence  
53 CUE<sup>22</sup>, and also because it is difficult to control for temperature-driven changes in nutrient availability  
54 in the medium<sup>5,19</sup>. This uncertainty about strain-level thermal responses of bacterial CUE severely limits  
55 our ability to understand responses of microbial populations to warming, and build mechanistic models  
56 of community-level responses.

57 Here, we quantify CUE using laboratory experiments at the level of single strains for 29 aerobic

58 environmental bacterial isolates spanning 9 families within 3 phyla. We combine this with a data-  
59 synthesis of > 400 growth and respiration thermal performance curves spanning most major culturable  
60 bacterial phyla<sup>23</sup>, to uncover general patterns in the temperature-dependence of CUE.

61 We first made precise the relationship between the thermal performance curve (TPC) of CUE and that  
62 of its underlying metabolic traits using a mathematical model (Methods). This model allows us to express  
63 the thermal sensitivity of CUE (its apparent activation energy,  $E_{\text{CUE}}$ ) as a function of the sensitivities  
64 of growth rate ( $\mu$ ) and respiration rate ( $R$ ) (as activation energies  $E_{\mu}$  and  $E_R$ , respectively) within the  
65 population's Operational Temperature Range (OTR) (Fig. 1A).  $E_{\text{CUE}}$  therefore describes a population's  
66 change in CUE with temperature across the OTR. Specifically, within the OTR, CUE decreases with  
67 temperature (negative  $E_{\text{CUE}}$ ) if the thermal sensitivity of respiration is greater than that of growth, and  
68 vice versa.

69 We then estimated  $E_R$  and  $E_{\mu}$  for each of the 29 bacterial strains by fitting the thermal response of  
70 growth and respiration rate within its OTR to the Boltzmann-Arrhenius TPC model (eq. 4) (Methods).  
71 To characterise the TPCs of the two traits, we measured growth and respiration rates at the same time-  
72 point of (exponential) population growth, over the same timescale, overcoming a key limitation of many  
73 previous such studies (Methods). Across our dataset, we find that the majority of strains (21/29) display  
74 a non-significant response of CUE to temperature within their OTR (Figs. 1B & 2). Seven strains show a  
75 significant increase in CUE with temperature, while only one strain shows a significant decrease in CUE  
76 with temperature (Figs. 1B & 2, Supplementary Table S2). Furthermore, we find that strains showing a  
77 positive CUE thermal response tend to be those with lower CUE in general, whilst the opposite is true  
78 for high efficiency strains (linear regression, intercept = 0.44, slope = -0.76,  $F_{1,27} = 10.86$ ,  $p = 0.0028$ ,  
79 Fig. 2B). Although by eye there appears to be some curvature, a straight line is preferred by AIC over a  
80 polynomial using linear regression. These responses are taxonomically structured, with lower efficiency  
81 *Proteobacteria* showing positive temperature responses and higher efficiency *Firmicutes* tending towards  
82 negative CUE thermal responses. Also, although the thermal optima for growth ( $T_{\text{pk},\mu}$ ) and respiration  
83 ( $T_{\text{pk},R}$ ) are highly correlated (Pearson's  $r = 0.91$ ), growth rates generally peak at lower temperatures than  
84 respiration rates ( $T_{\text{pk},\mu} < T_{\text{pk},R}$ , paired  $t_{23} = 4.996$ ,  $p < 0.001$  Fig. 3A). This validates our assumption  
85 of a monotonic CUE thermal response within the OTR (Fig. 1).

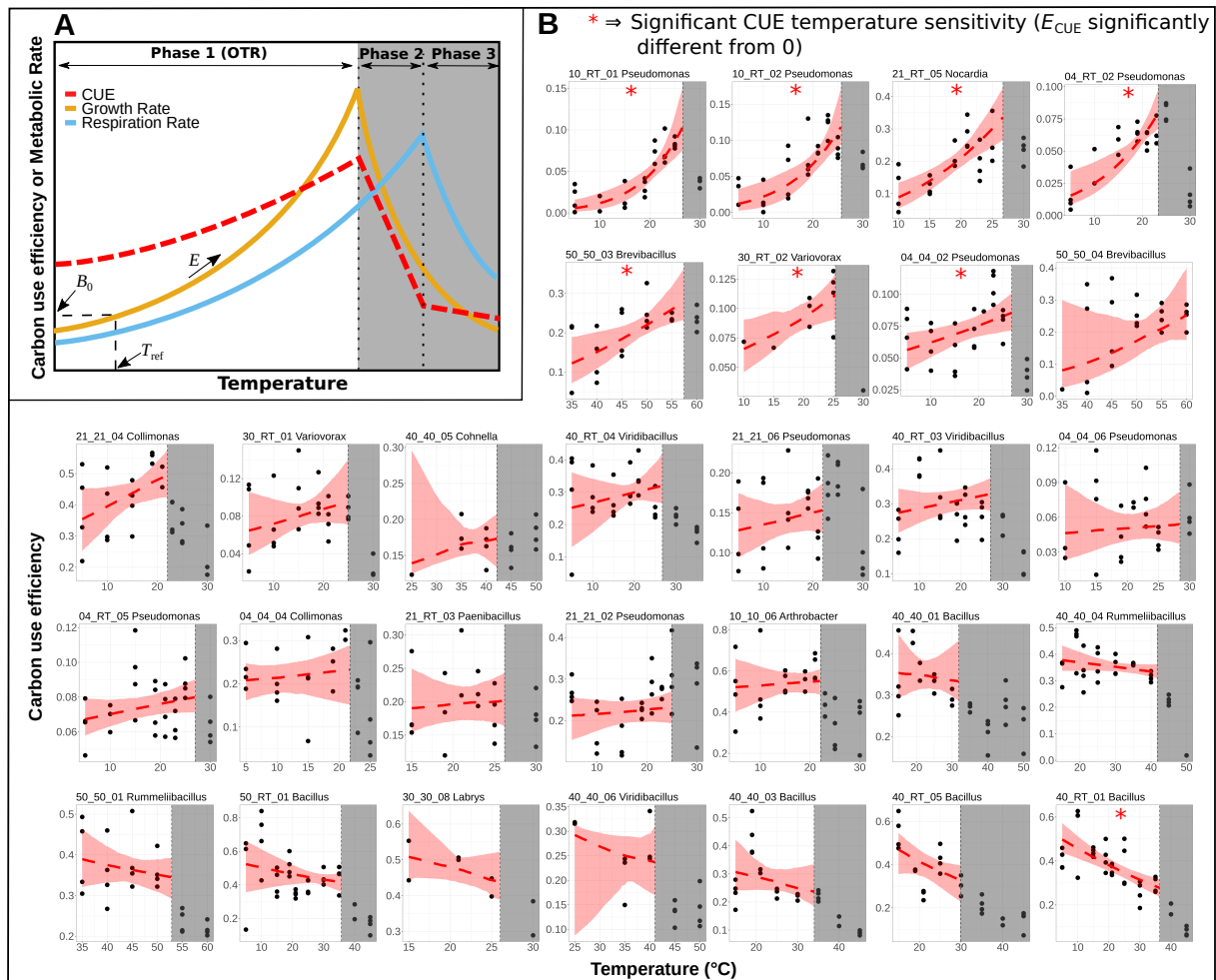


**Figure 1: The temperature dependence of carbon use efficiency** **A.** Growth (orange) and respiration (blue) show a unimodal thermal performance curve (TPC) with temperature. The portion of the TPC within the population’s operational temperature range (OTR)—the unshaded region—can be modelled using the Boltzmann-Arrhenius (BA) equation (eq. 4 in Methods; model parameters labeled on growth rate TPC). The upper limit of the OTR is defined by  $T_{pk,\mu}$ , the temperature at which growth rate peaks. The difference in BA equation parameters between growth and respiration determines the TPC of CUE (red dashed line). **B.** The TPCs of the within-OTR CUE for each of 29 bacterial strains (up to 4 replicates at each temperature). The header for each plot gives the strain ID code (Supplementary Table S1) and the bacterial genus. The red dashed line is the TPC of CUE within the OTR, calculated as the median of the responses of 1000 bootstrapped fits of the TPCs of  $\mu$  and  $R$  to the Boltzmann-Arrhenius model (Methods). The red shaded area is the (bootstrapped) 95% confidence envelope around the CUE TPC.

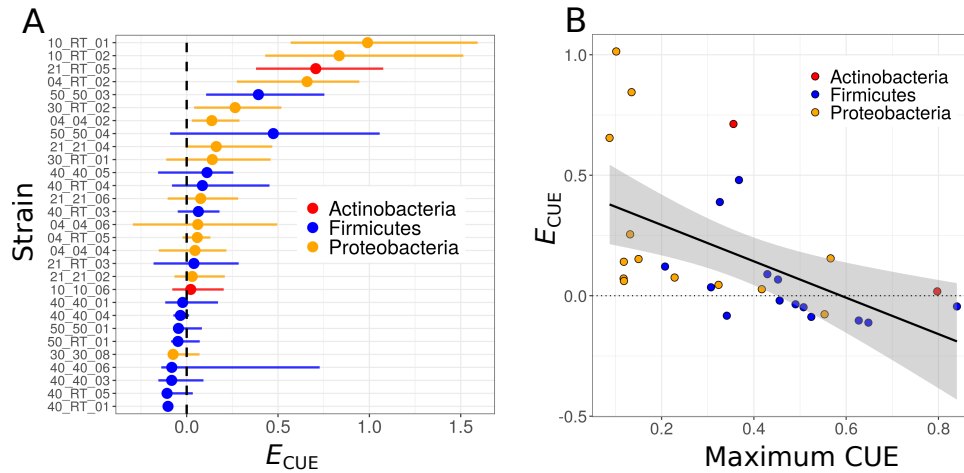


**Figure 2: The thermal sensitivity of CUE varies across bacterial taxa.** **A** Median bootstrapped  $E_{CUE}$  with 95% confidence intervals (CIs), strains ordered by the directionality of their response, from positive to negative, and coloured by phylum. Seven strains have a lower CI that falls above zero (black, dashed line), indicating a positive CUE thermal sensitivity within the OTR. The majority of strains' CIs include zero, indicating insignificant directionality (CUE TPC is thermally insensitive). A single strain "40\_RT\_01" displayed a significantly negative thermal response for CUE. **B** There is a significant negative relationship (linear regression  $p = 0.00275$ , black line with grey confidence envelope) between the measured CUE for each strain, and its CUE thermal sensitivity ( $E_{CUE}$ ), *i.e.*, less efficient strains are able to increase their efficiency with temperature, while high efficiency strains cannot.

86 The expectation for a decreasing CUE response to temperature is based on the assumption that respi-  
 87 ration is more sensitive to temperature (higher  $E$ ) than growth. However, given our theoretical analysis,  
 88 our empirical results imply higher sensitivity for growth in most cases (*i.e.*,  $E_{\mu} > E_R$ ; Fig 1). We in-  
 89 vestigated this further using our paired growth and respiration rate TPC data. Comparing the  $E_R$  and  
 90  $E_{\mu}$  values across strains, we find that whilst the two are positively correlated (Pearson's  $r = 0.432$ ), on  
 91 average,  $E_{\mu}$  is significantly greater than  $E_R$  (paired  $t_{28} = 2.513$ ,  $p = 0.009$ , Fig. 3B). To determine the  
 92 generality of our results, we next expanded our investigation of the difference between  $E_{\mu}$  and  $E_R$  using  
 93 a synthesis of published data spanning a much wider diversity of bacteria<sup>23</sup>. We find strikingly similar  
 94 differences in the shape of the distributions of  $E_{\mu}$  and  $E_R$  in our experimental (Fig. 3C) and literature  
 95 data (Fig. 3D), and find the same pattern of  $E_{\mu} > E_R$  on average within the data-synthesis TPCs  
 96 (median  $E_{\mu} = 0.84$ , median  $E_R = 0.66$ , Fig. 3D). Therefore, the CUE TPC is more likely to increase or  
 97 be thermally insensitive, than decrease within the OTR across bacteria in general.

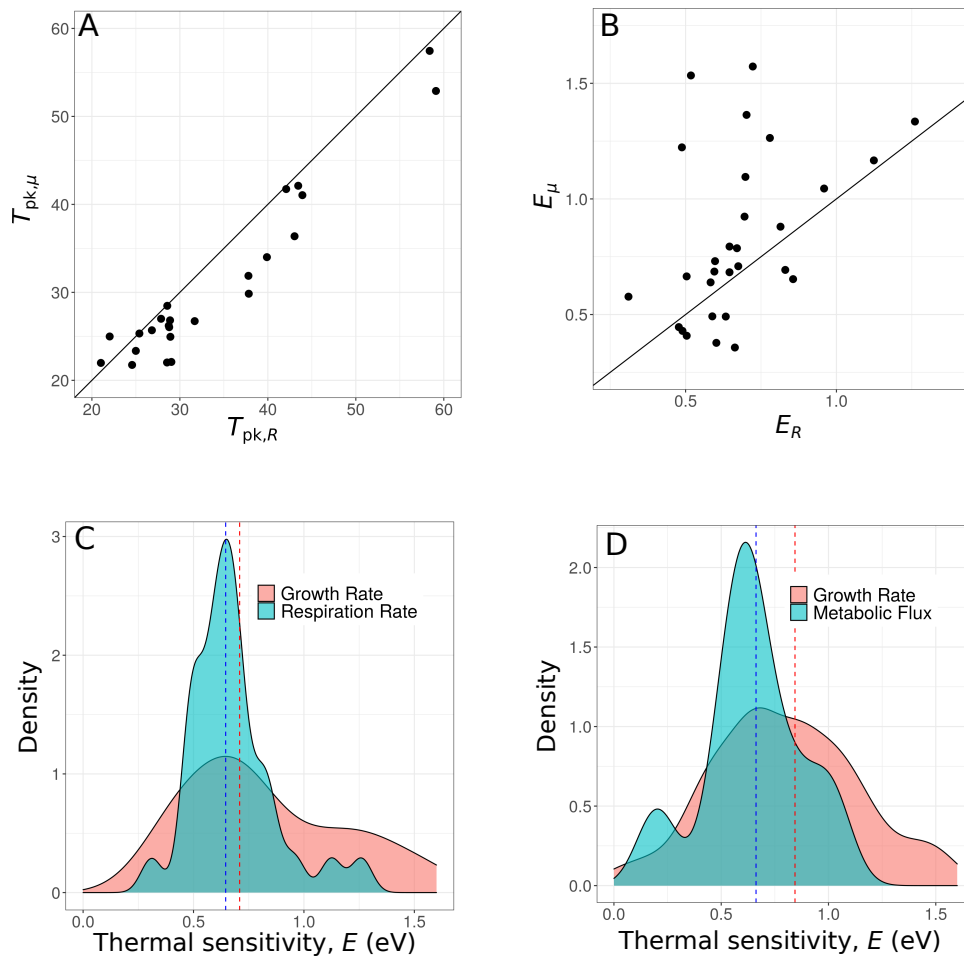


**Figure 3: Variation in TPC parameters.** **A** and **B** The relationship between growth rate and respiration rate for  $T_{pk}$  and thermal sensitivity ( $E$ ) respectively (1:1 lines shown). Datapoints are parameter estimates extracted from fits to empirical data ( $n = 29$ ). There are five fewer points for the  $T_{pk}$  comparison because one or both of the TPCs did not peak within the range of the data and thus  $T_{pk}$  could not be compared (however the thermal sensitivity,  $E$ , can still be estimated for these). **C** Distribution of  $E$  for growth rate and respiration rate in the experimental data. Red (growth rate) and blue (respiration rate) dotted lines show median values (median  $E_\mu = 0.71$ , median  $E_R = 0.65$ ). **D** Distribution of  $E$  for growth rate and metabolic flux rates (proxies for respiration) from a data-synthesis of  $> 400$  bacterial TPCs<sup>23</sup> (median  $E_\mu = 0.84$ , median  $E_R = 0.66$ ). Median  $E$  values in our experimentally-derived TPCs are lower than those in the data-synthesis because the former were estimated by fitting the Boltzmann-Arrhenius model and the latter using the Sharpe-Schoolfield model (Methods).

98 Our results yield a new understanding of the temperature dependence of microbial carbon use efficiency.  
 99 Our study on 29 strains of environmentally isolated aerobic bacteria combined with our data-synthesis  
 100 goes far beyond the scope of any previous culture-based studies into the temperature dependence of CUE  
 101 and its underlying traits. We find that CUE typically responds either positively to temperature, or is  
 102 invariant with temperature within the OTR (Fig. 2). Focusing on the OTR of each strain is key here,  
 103 as this is the temperature range within which the population typically operates, and only in the case of  
 104 extreme warming events would the CUE response beyond the OTR be relevant. This general pattern  
 105 in the CUE temperature dependence arises due to growth rate being typically more thermally sensitive  
 106 than respiration rate ( $E_\mu > E_R$ , Fig. 3B). Therefore, contrary to previous thinking, we conclude that

107 bacterial CUE generally increases or is invariant with temperature within strain-specific physiologically  
108 and ecologically meaningful temperature ranges.

109 The fact that growth rates generally peak at lower temperatures than respiration rates ( $T_{pk,\mu} < T_{pk,R}$ ,  
110 Fig. 3A) is in agreement with previous empirical studies at community<sup>24</sup>, as well as strain levels across  
111 both aerobic<sup>25,26</sup> and anaerobic<sup>27</sup> bacteria. Although the mechanistic basis for this systematic pattern  
112 is unclear, recent work suggests that it may be driven by stronger thermal constraints acting on carbon  
113 uptake and allocation rates, relative to respiration<sup>1,28</sup>. There is very little evidence in previous studies  
114 for the differences in thermal sensitivity ( $E$ ) of growth and respiration that we report here. Community  
115 respiration rates have in fact been reported to display higher thermal sensitivity than growth rate in  
116 aquatic systems<sup>14,18</sup>. However, it is difficult to disentangle the effect of nutrient limitation on growth  
117 versus respiration in community-level measurements of these rates, and it has been suggested that growth  
118 may be more nutrient limited than respiration in such settings<sup>5</sup>. Yet, a greater sensitivity of respiration  
119 relative to growth (and therefore, a negative response of CUE to temperature) is the assumption in most  
120 soil organic matter decomposition models<sup>3,4,15</sup>. Indeed, it is unclear why the growth and respiration  
121 responses should display differences in thermal sensitivity without the effects of nutrient limitation. If  
122 metabolic rate is a temperature dependent process, and biomass production is fueled by metabolism, it  
123 should follow that the temperature sensitivities of each should match<sup>29</sup>. However, although the responses  
124 of growth and respiration to temperature can be modelled on the basis of their responses being similar to  
125 a single rate-limiting enzymatic reaction<sup>30</sup>, these rates are in reality the end result of numerous complex  
126 biochemical and physiological processes, each with their own independent thermal sensitivities<sup>14,31</sup>. For  
127 aerobic heterotrophs, we may consider respiration rate to be equivalent to their “metabolic rate”, a  
128 process fundamentally dependent upon temperature<sup>31</sup>. Growth (or biomass production) however is a  
129 more emergent trait based on the fraction of metabolism allocated to it<sup>31</sup>. Given that the efficiency of  
130 allocation of carbon to growth varies with temperature in autotrophs<sup>28</sup>, a similar constraint may exist  
131 in heterotrophs.

132 We found a narrower distribution of  $E_R$  values than  $E_\mu$  (Fig. 3C). The differences in the shape of  
133 the distributions of  $E_R$  and  $E_\mu$  in our empirical results were also reflected in the global data-synthesis  
134 (Fig. 3D), implying that this phenomenon may be generalisable across the full taxonomic diversity of  
135 bacteria. The greater variability of  $E_\mu$  relative to  $E_R$  indicates that the generally positive CUE thermal  
136 response is partly due to the ability of bacterial populations to modify their carbon uptake rate and  
137 allocation efficiency for a given, constrained respiration rate. This also indicates stronger evolutionary as  
138 well as acclimation constraints acting upon the thermal sensitivity of respiration (the more fundamental  
139 metabolic process) than growth rate (the more emergent process), which can take a wider range of values.  
140 Indeed, recent work has shown that  $E_\mu$  can escape biophysical constraints and adapt to environmental

141 conditions<sup>32,33</sup>.

142 Theoretical calculations have placed maximum bacterial CUE at about 0.6<sup>34,35</sup>, and similar values  
143 have been reported from pure culture experiments (CUE = 0.6-0.85)<sup>2,36,37</sup>. A recent metabolic modelling  
144 study predicts variation in maximum CUE between taxa, with a range of 0.22 to 0.98 across different  
145 bacteria, with an average of  $\sim 0.62$ <sup>38</sup>. This theoretical variation is realised in the wide range of bacterial  
146 CUE values obtained from isolate experiments<sup>39</sup>. Generally lower CUE values are reported in natural  
147 systems than from isolate experiments<sup>39</sup>, from as low as 0.01 in the most dilute systems, to nearer 0.5  
148 in eutrophic systems<sup>10</sup>. The experimental data shown here fall very much within these ranges; for all  
149 recorded measurements across all experimental conditions, median CUE = 0.22, for only the maximal  
150 CUE values recorded from each strain, median CUE = 0.38 (see Supplementary Figure S2). We see a  
151 taxonomic divergence in these CUE measurements between the two main phyla in our empirical dataset,  
152 with *Firmicutes* tending towards high efficiency whilst *Proteobacteria* are generally less efficient (Figs.  
153 2 and S2). This is in agreement with recent work which suggests that closely related strains may have  
154 more similar CUE thermal responses than expected by chance (*i.e.*  $E_{\text{CUE}}$  is phylogenetically heritable)<sup>13</sup>.  
155 Furthermore, Pold *et al.*<sup>13</sup> show that the  $Q_{10}$  of CUE is higher for more efficient taxa which is analogous  
156 to our result of a negative relationship between  $E_{\text{CUE}}$  and maximum CUE. We find that this trade-off is  
157 well described as a linear relationship, with highly negative  $E_{\text{CUE}}$  values not being found, suggesting a  
158 potential biological limit. Our results have extended this understanding through a more precise estimation  
159 and generalisation of variation in  $E_{\text{CUE}}$ , via increased temperature measurements across strains adapted  
160 to a wider range of temperatures ( $T_{\text{pk},\mu}$  22°C - 57°C).

161 The overall magnitude of these CUE values are likely to be an over-estimate compared to the “real”  
162 growth efficiency calculated as the total carbon uptake allocated to growth. This is due to the implicit  
163 assumption of the commonly used CUE measure (Eqn. 2) that all carbon is allocated to either growth or  
164 respiration. In reality, there may be other avenues of carbon loss that are not visible to this experiment,  
165 such as excretion of metabolites. Whether this would cause a significant difference to these results of tem-  
166 perature dependent CUE would depend on whether excretion displays a pattern of temperature sensitivity  
167 distinct from respiration. The release of carbon by excretion is commonly assumed to be insignificant  
168 in models of bacterial growth<sup>40</sup>, however bacteria do excrete or leak metabolic by-products into the cul-  
169 ture medium<sup>1,40,41</sup>. In particular, with high levels of excess carbon in the substrate, some heterotrophic  
170 bacteria will excrete partially oxidised carbon into the environment in order to drain reducing power<sup>42</sup>.  
171 When nitrogen or phosphorous are the limiting nutrients and carbon levels are high, carbon excretion  
172 levels are high<sup>43</sup>. When carbon is the limiting nutrient however, levels of carbon excretion are much  
173 lower — Dauner *et al.*<sup>43</sup> report in the region of 3-6% of carbon uptake for *B. subtilis*. Our experimental  
174 data were derived from growth in the LB medium. This is a rich medium designed for exponential growth



175 under essentially nutrient-unlimited conditions. This was used to avoid the limitations of studies from  
176 natural systems, where nutrient limitation is likely to play a major role in the CUE response<sup>5</sup>. The most  
177 likely nutrient limiting growth in LB however is carbon<sup>44</sup> and therefore excretion is expected to account  
178 for only a small percentage of carbon loss. The results shown here are thus a reliable quantification of  
179 the temperature dependence of CUE in the absence of nutrient limitation.

180 Despite our empirical data being derived from lab experiments under nutrient saturated conditions,  
181 they represent a wide variety of strains isolated from environmental soil samples grown in a complex  
182 culture medium. Furthermore, we have extended these results to a data-synthesis spanning the entire  
183 taxonomic diversity of bacteria for which TPC data are available. Thus, our results are more generalisable,  
184 and applicable to real-world scenarios than previous culture-based experiments, which have tended to use  
185 lab-adapted strains grown on single carbon substrates, *e.g.* glucose. Our data are derived from cultures in  
186 exponential growth and therefore may provide a poor comparison to natural environments. These systems  
187 are often assumed to be at steady state, where CUE may be driven by maintenance metabolism of much  
188 lower turnover populations more generally. However, microbial systems may be more dynamic in nature,  
189 with repeated successional changes following environmental perturbations<sup>45</sup>. Furthermore, environments  
190 contain ‘hot-spots’ of microbial activity with much higher process rates than average conditions<sup>46</sup>, where  
191 exponential growth is relevant.

192 In conclusion, we have shown that, in contrast to current thinking, the response of bacterial CUE to  
193 temperature is generally invariant or positive within a biologically and ecologically relevant temperature  
194 range. This suggests that bacterial taxa are more robust to temperature change than is currently thought.  
195 These findings are important both, for physiologists aiming to understand abiotic effects on bacterial  
196 growth efficiency, as well as for parameterising ecosystem models for environment-driven variation in  
197 microbial carbon sequestration and efflux. In particular, re-parameterising microbial CUE in ecosystem  
198 models as an insensitive or increasing rather than decreasing function of temperature will likely have a  
199 major effect on predictions for both short-term responses of microbial community fluxes to temperature  
200 fluctuations, as well as longer term responses to climate change).

## 201 **Methods**

### 202 **Quantifying the temperature-dependence of CUE theoretically**

203 Here we make precise the relationship between the temperature-dependence of CUE and that of its underlying  
204 metabolic traits using a mathematical model. Consider a general equation for microbial population growth:

$$\frac{1}{C} \frac{dC}{dt} = \mu = \epsilon U;$$

205 where the change in population biomass,  $C$ , over time,  $t$ , (the growth rate,  $\mu$ ) is determined by the product  
206 of the carbon uptake rate,  $U$ , and an efficiency,  $\epsilon$ . This is the nutrient unlimited version of a more general  
207 growth equation appropriate for measurement of exponential population growth<sup>28,47</sup>. Although there may be  
208 other sources of carbon loss to a growing bacterial population such as metabolite excretion, we assume that the  
209 majority of carbon uptake is allocated to growth and respiration, *i.e.*  $U \approx R + \mu$ . Then,  $\epsilon$  can be expressed as:

$$210 \quad \epsilon = \frac{\mu}{\mu + R} = \text{CUE}. \quad (2)$$

211 This is the same CUE (carbon use efficiency) measure found throughout the bacterial literature<sup>1,2,4,11,35</sup> (eq.  
212 1), but this simple derivation makes explicit that the measure is meaningful only in the exponential growth phase  
213 of a population: it is (approximately) the proportion of carbon taken up by the cell that is allocated to growth  
214 during the exponential growth phase of the population.

215 Next, we consider how the TPC of CUE depends on TPCs of the underlying growth and respiration rates. The  
216 TPCs of a metabolic rate ( $B$ ) can be adequately modelled by using a simplified Sharpe-Schoolfield equation<sup>30</sup>  
217 obtained by dropping the low temperature inactivation and re-expressing the equation with  $T_{pk}$  as an explicit  
218 parameter<sup>23,33,48,49</sup>:

$$219 \quad B = B_0 \frac{e^{-\frac{E}{k} \cdot \left(\frac{1}{T} - \frac{1}{T_{ref}}\right)}}{1 + \frac{E}{E_D - E} e^{\frac{E_D}{k} \left(\frac{1}{T_{pk}} - \frac{1}{T}\right)}} \quad (3)$$

220 Here,  $T$  is temperature in Kelvin (K),  $B$  is a biological rate,  $B_0$  is the rate at a low reference temperature  
221 ( $T_{ref}$ ),  $E$  is the activation energy (eV),  $E_D$  the deactivation energy that determines the rate of decline in the  
222 biological rate beyond the temperature of peak rate ( $T_{pk}$ ), and  $k$  is the Boltzmann constant ( $8.617 \times 10^{-5}$  eV  
223  $K^{-1}$ ). The temperature-independent constant  $B_0$  includes the scaling effect of cell size, which we ignore here  
224 as cell size variation is not relevant for understanding the shape of the TPC of CUE (assuming cell size does  
225 not change significantly in the timescale over which CUE is measured). Substituting the full TPCs of  $\mu$  and  $R$   
226 defined using eq. 3 into eq. 2 can be used to quantify the CUE TPC, and can result in a large array of shapes  
227 depending upon the parameters of the  $\mu$  and  $R$  TPCs (Supplementary Figure S3). However, the entire range of  
228 temperatures spanned by the TPCs of  $\mu$  and  $R$  in eq. 3 are not biologically relevant because organisms generally  
229 live within their “Operational Temperature Range”(OTR), defined as the temperature range from some lower  
230 critical temperature (*e.g.*,  $0^\circ\text{C}$ ) and the temperature of peak fitness  $\mu$  (henceforth denoted by  $T_{pk,\mu}$ )<sup>50,51</sup> (the  
231 “Phase 1” range in Fig. 1A). Additional phases of the TPCs of  $\mu$ ,  $R$  and CUE can also be identified — the range  
232 between the temperature of peak  $\mu$  and peak  $R$  and that beyond the peak of  $R$  (Phase 2 and 3 respectively in  
233 Fig. 1A) — but these are also not relevant here. Within this OTR the TPCs of  $\mu$  and  $R$  can be modelled simply  
234 using the Boltzmann-Arrhenius function<sup>23,30,51,52</sup>, eq 4 (the numerator of eq. 2):

$$235 \quad B(T) = B_0 e^{-\frac{E}{k} \cdot \left(\frac{1}{T} - \frac{1}{T_{ref}}\right)}, \quad (4)$$

236 This assumes that neither growth nor respiration peak within the OTR. Indeed, growth cannot peak within  
237 the OTR by definition, as this is the range from the minimum growth temperature up to the peak growth

238 temperature<sup>51</sup>. Therefore to use the Boltzmann-Arrhenius function here, we must also assume that respiration  
 239 generally peaks at higher temperatures than growth, as has previously been suggested<sup>1,24</sup>. This expectation is  
 240 observed within our dataset of empirical TPCs (see supplementary information). Therefore within the OTR (the  
 241 typically-experienced temperature range for a strain), we can define an expression for CUE by using Boltzmann-  
 242 Arrhenius functions (eq. 4) for growth ( $\mu$ ) and respiration ( $R$ ) respectively, to give:

$$243 \quad \text{CUE} = \frac{\mu_0 e^{-\frac{E_\mu}{k} \cdot \left(\frac{1}{T} - \frac{1}{T_{\text{ref}}}\right)}}{\mu_0 e^{-\frac{E_\mu}{kT} \cdot \left(\frac{1}{T} - \frac{1}{T_{\text{ref}}}\right)} + R_0 e^{-\frac{E_R}{kT} \cdot \left(\frac{1}{T} - \frac{1}{T_{\text{ref}}}\right)}}. \quad (5)$$

244 The simplification of equation 5 yields a CUE function which is monotonic over the OTR, with a direction  
 245 defined entirely by differences in  $E_\mu$  and  $E_R$ . If  $E_\mu > E_R$ , CUE rises with temperature over the OTR, if  $E_\mu < E_R$ ,  
 246 CUE declines with temperature across the OTR. This is the basis for previous theoretical expectations for the  
 247 CUE temperature response<sup>1</sup>, here formalised as eq. 5. Specifically, we can approximate the denominator in eq.  
 248 5 using a Taylor series expansion, to obtain the following approximation for CUE:

$$249 \quad \text{CUE} \approx \frac{\mu_0 e^{\left(-E_\mu + \frac{E_R R_0 + E_\mu \mu_0}{R_0 + \mu_0}\right) \cdot \left(\frac{1}{T} - \frac{1}{T_{\text{ref}}}\right)}}{R_0 + \mu_0}. \quad (6)$$

250 This equation has the form of a Boltzmann-Arrhenius function with:

$$251 \quad B_0 = \frac{\mu_0}{\mu_0 + R_0} \quad (7)$$

252 and the apparent activation energy (a measure of thermal sensitivity of CUE) as

$$253 \quad E_{\text{CUE}} = E_\mu - \frac{E_\mu \mu_0 + E_R R_0}{\mu_0 + R_0}. \quad (8)$$

254 Thus, the CUE TPC is necessarily monotonic within the OTR as long as  $T_{\text{pk},\mu} < T_{\text{pk},R}$  (as is almost always  
 255 the case; see Fig. 3).

256 This expression can be used to determine the direction of the CUE thermal sensitivity within the OTR as  
 257 follows. Recognising that the condition for CUE to decrease with temperature is  $E_{\text{CUE}} < 0$ , we can rearrange eq  
 258 8 as :

$$E_\mu < \frac{E_\mu \mu_0 + E_R R_0}{\mu_0 + R_0}$$

259 This simplifies to the condition

$$E_\mu < E_R.$$

260 That is, within the OTR, CUE increases if  $E_R < E_\mu$  ( $\implies E_{\text{CUE}} > 0$ ), decreases if  $E_R > E_\mu$  ( $\implies E_{\text{CUE}} < 0$ ),  
 261 and is insensitive to temperature if  $E_R = E_\mu$  ( $\implies E_{\text{CUE}} = 0$ )

## 262 Quantifying the temperature dependence of CUE experimentally

263 We used 29 strains of environmentally isolated aerobic bacteria from our laboratory culture collection (see sup-  
264 plementary table S1). These strains were isolated under a range of different temperatures for a species sorting  
265 experiment, aiming to reconstruct the wide diversity of bacterial temperature fitness present in soils. We experi-  
266 mentally quantified the TPC of CUE for these bacteria as follows.

267 At each experimental temperature, frozen bacterial cultures were revived and grown to carrying capacity at the  
268 experimental temperature (acclimation period - to restrict influence of temperature stress on TPC, or equalise  
269 it across experimental points). Revived cultures were grown in LB medium in replicates of 4 and growth rate  
270 and respiration rate were measured during exponential growth using flow cytometry cell counts (growth) and  
271 MicroResp™ (respiration). This was repeated across a range of temperatures spanning the full TPC for each  
272 isolate.

273 From the flow cytometry measurements, estimates of carbon biomass in the cultures were made based on cell  
274 diameters<sup>53</sup>, and growth in the exponential phase calculated as:

$$275 \mu = \frac{\log\left(\frac{C_1}{C_0}\right)}{t}; \quad (9)$$

276 where  $C_0$  is the starting biomass,  $C_1$  is the final biomass and  $t$  is the duration of the experiment. MicroResp™  
277 was used to give a quantitative measure of the cumulative respired CO<sub>2</sub> produced during the growth experiment<sup>54</sup>.  
278 From this, the per-capita respiration rate was calculated in terms of carbon mass, according to:

$$279 R = \frac{\mu R_{tot}}{C_0 e^{\mu t} - C_0}. \quad (10)$$

280 Here,  $R_{tot}$  is the total mass of carbon produced,  $C_0$  is the initial population biomass,  $\mu$  is the previously  
281 calculated growth rate and  $t$  is the duration of the experiment (see supplementary material for full details of the  
282 derivation of eq 10). This measure of respiration rate is directly comparable to the specific growth rate,  $\mu$ , and  
283 overcomes a problem shared by practically all previous empirical measurements of CUE. Specifically, for a given  
284 temperature, previous methods have often required growth rates to be measured at a different timescale, or at  
285 a different time point of population growth, than the measurement of respiration rate. This is because  $\mu$  needs  
286 to be measured over time-period sufficiently long enough to allow changes in cell density to be detectable using  
287 optical methods, while respiration rate can be measured over much shorter timescales. The resulting difference  
288 in timescales of measurement permits a greater level of thermal acclimation of growth relative to respiration.  
289 Furthermore, in cases where these measurements *have* been made over a similar time-frame, respiration rates  
290 are often normalised only to the starting mass of the growing population, and neglect to include changes in  
291 the growing population size over time (*e.g.* Keiblinger *et al.*<sup>11</sup>, Créach *et al.*<sup>55</sup>, Warkentin *et al.*<sup>56</sup>). Indeed,  
292 direct comparisons of the TPCs of growth and respiration that our methods allow have largely been lacking  
293 from the literature, making it difficult to link these processes to temperature-dependent CUE at the appropriate  
294 timescale<sup>57</sup>.

## 295 **Calculating CUE from the experimental data**

296 Having measured the TPCs of growth and respiration rate, we then calculated the within-OTR TPC of CUE for  
297 each bacterial strain as follows. We first fit the Sharpe-Schoolfield model (eq. 3, Methods) to paired growth rate  
298 and respiration rate TPCs for each of the 29 strains of aerobic bacteria to determine the respective  $T_{pk,\mu}$  and  
299  $T_{pk,R}$ , and then fitted the Boltzmann-Arrhenius model (eq. 4) to the TPC from the rate at minimum temperature  
300 up to its  $T_{pk}$ . To fit eq. 4 to the temperature dependent growth and respiration rates to each of the 29 strains in  
301 our dataset, we used only those strains that had at least 3 datapoints in the temperature range lower than their  
302 Shape-Schoolfield calculated  $T_{pk}$ . We input these TPC parameters for  $\mu$  and  $R$  (calculated from eq. 4) into eq.  
303 5 to calculate the CUE TPC, and its corresponding  $E_{CUE}$  using eq. 8. All analyses and model fitting were  
304 performed in R<sup>58</sup>, using the “minpack.lm” package for non-linear least squares fitting.

## 305 **Accounting for uncertainty in model fitting**

306 To account for uncertainty in the estimated TPCs (*i.e.*, in the parameters  $B_0$  and  $E$ ; eq. 4) in our tests of  
307 whether the emergent CUE responds significantly to temperature, we implemented a bootstrapping approach as  
308 follows. For each strain we re-sampled the data with replacement 1,000 times and re-fit the Boltzmann-Arrhenius  
309 model (eq. 4) to the sub-sampled growth and respiration dataset. As the data are paired (each CUE value  
310 is derived from a growth and a respiration measurement), we re-sampled growth and respiration paired points  
311 (rather than re-sampling growth and respiration separately), in order to account for their covariance. From each  
312 of the paired BA model fits we calculated  $E_{CUE}$  according to eq. 8, obtaining a distribution of these values. We  
313 then calculated the 95% confidence interval for  $E_{CUE}$  as the 2.5th and 97.5th percentiles of this distribution. We  
314 asked whether or not the CIs include zero, as a robust test to determine a thermal response significantly different  
315 from a temperature insensitive response (Fig. 2).

316 In order to calculate a confidence envelope around each CUE TPC, we took the fitted parameters from the  
317 1,000 bootstrapped curves for each strain and interpolated CUE curves across the temperature range for plotting.  
318 At each temperature, we took the 2.5th and 97.5th percentiles of the CUE distribution as the upper and lower  
319 bounds of the 95% confidence envelope.

## 320 **Data-synthesis of bacterial thermal performance curves**

321 To understand our results in a broader context, we compared the thermal sensitivities of our empirically derived  $\mu$   
322 and  $R$  TPCs to those in our recent global data synthesis<sup>23</sup>. This data synthesis is primarily composed of growth  
323 rate TPCs (416 bacterial  $\mu$  TPCs), but also contains 22 bacterial metabolic flux TPCs which we use as proxies for  
324 respiration rate TPCs. This is a taxonomically and functionally diverse dataset, spanning 13 bacterial phyla and  
325 practically the entire range of thermal niches inhabited by bacteria. Rather than re-analyse the raw data here,  
326 we directly take the  $E_\mu$  and  $E_R$  estimates provided and compare the distributions to those of our empirically  
327 derived TPCs. The data-synthesis calculates  $E$  directly from the Sharpe-Schoolfield model (eq. 3), whereas here  
328 we calculate  $E$  from the Boltzmann-Arrhenius function (eq. 4) fitted within the OTR. This is expected to cause a  
329 difference in the overall magnitude of  $E$  between datasets (lower  $E$  using Boltzmann-Arrhenius due to curvature

330 as trait values approach  $T_{pk}^{51}$ ), however we emphasise this does not affect  $E_{\mu}$  and  $E_R$  comparisons within these  
331 datasets, nor the comparison of distributions between these datasets.

## 332 Acknowledgements

333 TPS was supported by a BBSRC DTP scholarship (BB/J014575/1). TB and SP were funded by NERC grants  
334 NE/M020843/1 and NE/S000348/1.

## 335 References

- 336 1. Manzoni, S., Taylor, P., Richter, A., Porporato, A. & Ågren, G. I. Environmental and stoichiometric controls  
337 on microbial carbon-use efficiency in soils. *New Phytologist* **196**, 79–91 (2012).
- 338 2. Geyer, K. M., Kyker-Snowman, E., Grandy, A. S. & Frey, S. D. Microbial carbon use efficiency: account-  
339 ing for population, community, and ecosystem-scale controls over the fate of metabolized organic matter.  
340 *Biogeochemistry* **127**, 173–188 (2016).
- 341 3. Allison, S. D., Wallenstein, M. D. & Bradford, M. A. Soil-carbon response to warming dependent on microbial  
342 physiology. *Nature Geoscience* **3**, 336–340 (2010).
- 343 4. Allison, S. D. Modeling adaptation of carbon use efficiency in microbial communities. *Frontiers in Microbiology*  
344 **5**, 1–9 (2014).
- 345 5. Lopez-Urrutia & Moran, X. A. G. Resource Limitation of Bacterial Production Distorts the Temperature  
346 Dependence Of Oceanic Carbon Cycling. *Ecology* **88**, 817–822 (2007).
- 347 6. Geyer, K. M., Dijkstra, P., Sinsabaugh, R. & Frey, S. D. Clarifying the interpretation of carbon use efficiency  
348 in soil through methods comparison. *Soil Biology and Biochemistry* **128**, 79–88 (2019).
- 349 7. Frey, S. D., Lee, J., Melillo, J. M. & Six, J. The temperature response of soil microbial efficiency and its  
350 feedback to climate. *Nature Climate Change* **3**, 395–398 (2013).
- 351 8. Fatichi, S., Manzoni, S., Or, D. & Paschalis, A. A Mechanistic Model of Microbially Mediated Soil Biogeo-  
352 chemical Processes: A Reality Check. *Global Biogeochemical Cycles* **33**, 620–648 (2019).
- 353 9. Dunne, J. P., Armstrong, R. A., Gnnadesikan, A. & Sarmiento, J. L. Empirical and mechanistic models for  
354 the particle export ratio. *Global Biogeochemical Cycles* **19** (2005).
- 355 10. del Giorgio, P. A. & Cole, J. J. Bacterial Growth Efficiency in Natural Aquatic Systems. *Annual Review of*  
356 *Ecology and Systematics* **29**, 503–541 (1998).
- 357 11. Keiblinger, K. M. *et al.* The effect of resource quantity and resource stoichiometry on microbial carbon-use-  
358 efficiency. *FEMS Microbiology Ecology* **73**, 430–440 (2010).

- 359 12. Zheng, Q. *et al.* Growth explains microbial carbon use efficiency across soils differing in land use and geology.  
360 *Soil Biology and Biochemistry* **128**, 45–55 (2019).
- 361 13. Pold, G. *et al.* Carbon use efficiency and its temperature sensitivity covary in soil bacteria. *mBio* **11**,  
362 e02293–19 (2020).
- 363 14. Apple, J. K., del Giurgi, P. A. & Kemp, W. M. Temperature regulation of bacterial production, respiration,  
364 and growth efficiency in a temperate salt-marsh estuary. *Aquatic Microbial Ecology* **43**, 243–254 (2006).
- 365 15. Schimel, J. P. & Weintraub, M. N. The implications of exoenzyme activity on microbial carbon and nitrogen  
366 limitation in soil: A theoretical model. *Soil Biology and Biochemistry* **35**, 549–563 (2003).
- 367 16. Steinweg, J. M., Plante, A. F., Conant, R. T., Paul, E. A. & Tanaka, D. L. Patterns of substrate utilization  
368 during long-term incubations at different temperatures. *Soil Biology and Biochemistry* **40**, 2722–2728 (2008).
- 369 17. Qiao, Y. *et al.* Global variation of soil microbial carbon-use efficiency in relation to growth temperature and  
370 substrate supply. *Scientific Reports* **9**, 1–8 (2019).
- 371 18. Rivkin, R. B., Legendre, L., Enquist, B. J., Savage, V. M. & Charnov, E. L. Biogenic Carbon Cycling in the  
372 Upper Ocean: Effects of Microbial Respiration. *Science* **291**, 2398–2400 (2001).
- 373 19. Dijkstra, P. *et al.* Effect of temperature on metabolic activity of intact microbial communities: Evidence for  
374 altered metabolic pathway activity but not for increased maintenance respiration and reduced carbon use  
375 efficiency. *Soil Biology and Biochemistry* **43**, 2023–2031 (2011).
- 376 20. Hagerty, S. B. *et al.* Accelerated microbial turnover but constant growth efficiency with warming in soil.  
377 *Nature Climate Change* **4**, 903–906 (2014).
- 378 21. Öquist, M. G. *et al.* The effect of temperature and substrate quality on the carbon use efficiency of saprotrophic  
379 decomposition. *Plant and Soil* **414**, 113–125 (2017).
- 380 22. Domeignoz-Horta, L. A. *et al.* Microbial diversity drives carbon use efficiency in a model soil. *Nature*  
381 *Communications* **11**, 3684 (2020).
- 382 23. Smith, T. P. *et al.* Community-level respiration of prokaryotic microbes may rise with global warming. *Nature*  
383 *Communications* **10**, 5124 (2019).
- 384 24. Pietikäinen, J., Pettersson, M. & Bååth, E. Comparison of temperature effects on soil respiration and bacterial  
385 and fungal growth rates. *FEMS Microbiology Ecology* **52**, 49–58 (2005).
- 386 25. Christian, R. R. & Wiebe, W. J. The effects of temperature upon the reproduction and respiration of a  
387 marine obligate psychrophile. *Canadian Journal of Microbiology* **20**, 1341–1345 (1974).
- 388 26. Kusnetsov, J. M., Ottoila, E. & Martikainen, P. J. Growth, respiration and survival of *Legionella pneumophila*  
389 at high temperatures. *Journal of Applied Bacteriology* **81**, 341–347 (1996).

- 390 27. Knoblauch, C. & Jorgensen, B. B. Effect of temperature on sulphate reduction, growth rate and growth  
391 yield in five psychrophilic sulphate-reducing bacteria from Arctic sediments. *Environmental Microbiology* **1**,  
392 457–467 (1999).
- 393 28. García-Carreras, B. *et al.* Role of carbon allocation efficiency in the temperature dependence of autotroph  
394 growth rates. *Proceedings of the National Academy of Sciences* **115**, E7361–E7368 (2018).
- 395 29. Luhring, T. M. & Delong, J. P. Scaling from Metabolism to Population Growth Rate to Understand How  
396 Acclimation Temperature Alters Thermal Performance. *Integrative and Comparative Biology* **57**, 103–111  
397 (2017).
- 398 30. Schoolfield, R. M., Sharpe, P. J. & Magnuson, C. E. Non-linear regression of biological temperature-dependent  
399 rate models based on absolute reaction-rate theory. *Journal of theoretical biology* **88**, 719–31 (1981).
- 400 31. Brown, J. H., Gillooly, J. F., Allen, A. P., Savage, V. M. & West, G. B. Toward a metabolic theory of ecology.  
401 *Ecology* **85**, 1771–1789 (2004).
- 402 32. Kontopoulos, D. G., Smith, T. P., Barraclough, T. G. & Pawar, S. Adaptive evolution explains the present-day  
403 distribution of the thermal sensitivity of population growth rate. *bioRxiv* (2019).
- 404 33. Kontopoulos, D. G. *et al.* Phytoplankton thermal responses adapt in the absence of hard thermodynamic  
405 constraints. *Evolution* (2020).
- 406 34. Roels, J. A. Application of Macroscopic Principles To Microbial Metabolism. *Biotechnology and bioengineering*  
407 2457–2514 (1980).
- 408 35. Sinsabaugh, R. L., Manzoni, S., Moorhead, D. L. & Richter, A. Carbon use efficiency of microbial communi-  
409 ties: Stoichiometry, methodology and modelling. *Ecology Letters* **16**, 930–939 (2013).
- 410 36. Gommers, P., van Schie, B., van Dijken, J. & Kuenen, J. Biochemical Limits to Microbial Growth Yields:  
411 An Analysis of Mixed Substrate Utilization. *Biotechnology and Bioengineering* **32**, 86–94 (1988).
- 412 37. Babel, W. The Auxiliary Substrate Concept: From simple considerations to heuristically valuable knowledge.  
413 *Engineering in Life Sciences* **9**, 285–290 (2009).
- 414 38. Saifuddin, M., Bhatnagar, J. M., Segrè, D. & Finzi, A. C. Microbial carbon use efficiency predicted from  
415 genome-scale metabolic models. *Nature Communications* **10** (2019).
- 416 39. Manzoni, S. *et al.* Reviews and syntheses : Carbon use efficiency from organisms to ecosystems definitions ,  
417 theories, and empirical evidence. *Biogeosciences* 5929–5949 (2018).
- 418 40. Touratier, F., Legendre, L. & Vézina, A. Model of bacterial growth influenced by substrate C:N ratio and  
419 concentration. *Aquatic Microbial Ecology* **19**, 105–118 (1999).
- 420 41. Russell, J. B. & Cook, G. M. Energetics of bacterial growth: balance of anabolic and catabolic reactions.  
421 *Microbiological reviews* **59**, 48–62 (1995).



- 422 42. Braakman, R., Follows, M. J. & Chisholm, S. W. Metabolic evolution and the self-organization of ecosystems.  
423 *Proceedings of the National Academy of Sciences* **114**, E3091–E3100 (2017).
- 424 43. Dauner, M., Storni, T. & Sauer, U. Bacillus subtilis Metabolism and Energetics in Carbon-Limited and  
425 Excess-Carbon Chemostat Culture. *Journal of Bacteriology* **183**, 7308–7317 (2001).
- 426 44. Sezonov, G., Joseleau-Petit, D. & D’Ari, R. Escherichia coli physiology in Luria-Bertani broth. *Journal of*  
427 *Bacteriology* **189**, 8746–8749 (2007).
- 428 45. Rivett, D. W. *et al.* Elevated success of multispecies bacterial invasions impacts community composition  
429 during ecological succession. *Ecology Letters* **21**, 516–524 (2018).
- 430 46. Kuzyakov, Y. & Blagodatskaya, E. Microbial hotspots and hot moments in soil: Concept & review. *Soil*  
431 *Biology and Biochemistry* **83**, 184–199 (2015).
- 432 47. Bestion, E., Garcia-Carreras, B., Schaum, C.-E., Pawar, S. & Yvon-Durocher, G. Metabolic traits predict  
433 the effects of warming on phytoplankton competition. *Ecology Letters* 1–10 (2018).
- 434 48. Padfield, D., Yvon-durocher, G., Buckling, A., Jennings, S. & Yvon-durocher, G. Rapid evolution of metabolic  
435 traits explains thermal adaptation in phytoplankton. *Ecology letters* 133–142 (2016).
- 436 49. Barton, S. *et al.* Evolutionary temperature compensation of carbon fixation in marine phytoplankton. *Ecology*  
437 *Letters* (2020).
- 438 50. Huey, R. B. & Kingsolver, J. G. Evolution of thermal sensitivity of ectotherm performance. *Trends in ecology*  
439 *& evolution* **4**, 131–5 (1989).
- 440 51. Pawar, S., Dell, A. I., Savage, V. M. & Knies, J. L. Real versus Artificial Variation in the Thermal Sensitivity  
441 of Biological Traits. *The American Naturalist* **187** (2016).
- 442 52. Dell, A. I., Pawar, S. & Savage, V. M. Systematic variation in the temperature dependence of physiological  
443 and ecological traits. *Proceedings of the National Academy of Sciences of the United States of America* **108**,  
444 10591–10596 (2011).
- 445 53. Romanova, N. D. & Sazhin, A. F. Relationships between the cell volume and the carbon content of bacteria.  
446 *Oceanology* **50**, 522–530 (2010).
- 447 54. Campbell, C. D., Chapman, S. J., Cameron, C. M., Davidson, M. S. & Potts, J. M. A rapid microtiter  
448 plate method to measure carbon dioxide evolved from carbon substrate amendments so as to determine  
449 the physiological profiles of soil microbial communities by using whole soil. *Applied and Environmental*  
450 *Microbiology* **69**, 3593–3599 (2003).
- 451 55. Créach, V., Baudoux, A. C., Bertru, G. & Rouzic, B. L. Direct estimate of active bacteria: CTC use and  
452 limitations. *Journal of Microbiological Methods* **52**, 19–28 (2003).

- 453 56. Warkentin, M., Freese, H. M., Karsten, U. & Schumann, R. New and fast method to quantify respiration  
454 rates of bacterial and plankton communities in freshwater ecosystems by using optical oxygen sensor spots.  
455 *Applied and Environmental Microbiology* **73**, 6722–6729 (2007).
- 456 57. Sinsabaugh, R. L., Shah, J. J., Findlay, S. G., Kuehn, K. A. & Moorhead, D. L. Scaling microbial biomass,  
457 metabolism and resource supply. *Biogeochemistry* **122**, 175–190 (2015).
- 458 58. R Core Team. R: A Language and Environment for Statistical Computing (2020).